

Solvation Effects on Wavenumbers and Absorption Intensities of the OH-Stretch Vibration in Phenolic Compounds – Electrical- and Mechanical Anharmonicity *via* a combined DFT/Numerov Approach – Supporting Information

*Manuel J. Schuler and Thomas S. Hofer**

Theoretical Chemistry Division, Institute of General, Inorganic and Theoretical Chemistry
Center for Chemistry and Biomedicine
University of Innsbruck, Innrain 80-82, A-6020 Innsbruck, Austria
Tel.: +43-512-507-57111, Fax: +43-512-507-57199

Yusuke Morisawa

Department of Chemistry
School of Science and Engineering, Kindai University, Kowakae
Higashi-Osaka, Osaka, 577-8502, Japan
Tel.: +81-0965-53-1211, Fax: +81-0965-53-1219

Yoshisuke Futami

Department of Biological and Chemical Systems Engineering
National Institute of Technology, Kumamoto College,
Yatsushiro, Kumamoto, 866-8501, Japan
Tel.: +81-0965-53-1211, Fax: +81-0965-53-1219

Christian W. Huck

Institute of Analytical Chemistry and Radiochemistry

Center for Chemistry and Biomedicine

University of Innsbruck, Innrain 80-82, A-6020 Innsbruck, Austria

Tel.: +43-512-507-57304, Fax: +43-512-507-53399

Yukihiro Ozaki[†]

Department of Chemistry,

School of Science and Technology

Kwansei Gakuin University, Sanda, Hyogo 669-1337, Japan

Tel.: +81-798-71-5206, Fax: +81-798-71-5206

May 13, 2020

*Corresponding author (theoretical) – E-Mail: t.hofer@uibk.ac.at

[†]Corresponding author (experimental) – E-Mail: yukiz89016@gmail.com

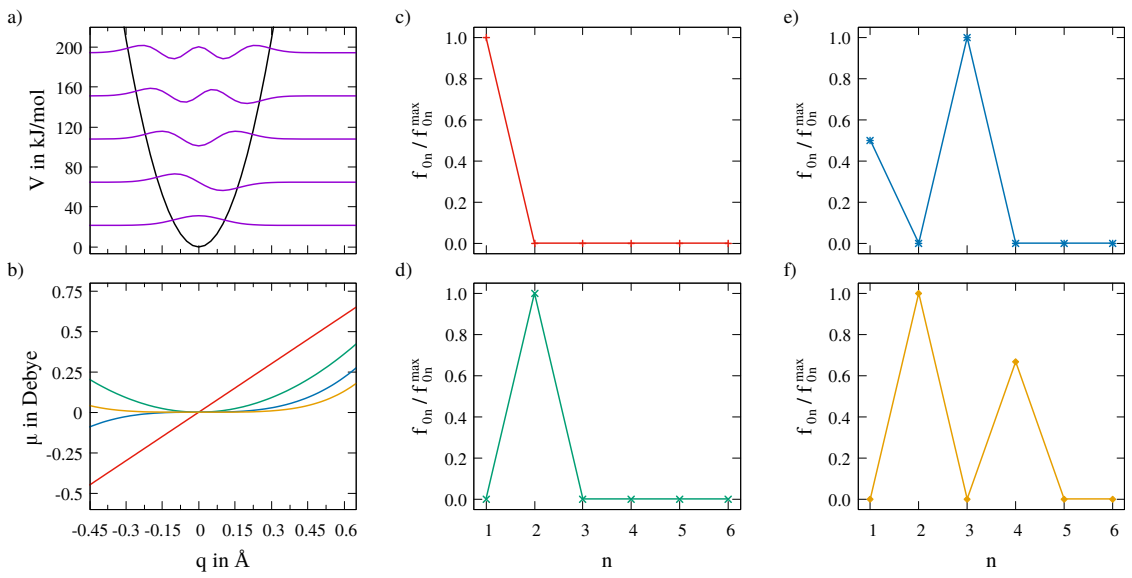


Figure S1: a) Potential (black) and vibrational eigenstates (purple) of the harmonic oscillator. b) Dipole moment change with idealised linear (red), quadratic (green), cubic (blue) and quartic (orange) dependence. c) to f) Oscillator strengths normalised to their respective largest values (f_{0n}/f_{0n}^{\max}) for the linear (c), quadratic (d), cubic (e) and quartic (f) dipole moment curves.

Table S1: Wavenumbers ν_{0n} in cm^{-1} and associated oscillator strengths f_{0n} obtained via the Numerov approach at B3LYP/6-311++G(3df,3pd) level in different environments for phenol with and without dispersion correction GD3BJ applied.

	n	Vacuum			CCl ₄			n-Hexane		
		Implicit		Explicit		Implicit		Explicit		
		ν_{0n}	f_{0n}	ν_{0n}	f_{0n}	ν_{0n}	f_{0n}	ν_{0n}	f_{0n}	f_{0n}
Phenol B3LYP	1	3665	$9.76 \cdot 10^{-6}$	36337	$1.70 \cdot 10^{-5}$	3632	$3.78 \cdot 10^{-5}$	3642	$1.54 \cdot 10^{-5}$	3664 $\cdot 10^{-6}$
	2	7167	$8.78 \cdot 10^{-7}$	7111	$9.62 \cdot 10^{-7}$	7094	$6.23 \cdot 10^{-7}$	7122	$9.44 \cdot 10^{-7}$	7166 $\cdot 10^{-7}$
	3	10513	$5.20 \cdot 10^{-8}$	10431	$6.16 \cdot 10^{-8}$	10392	$5.07 \cdot 10^{-8}$	10447	$6.04 \cdot 10^{-8}$	10511 $\cdot 10^{-8}$
	4	13705	$4.07 \cdot 10^{-9}$	13599	$6.40 \cdot 10^{-9}$	13529	$4.91 \cdot 10^{-9}$	13621	$6.15 \cdot 10^{-9}$	13703 $\cdot 10^{-9}$
Phenol B3LYP + GD3BJ	1	3664	$9.47 \cdot 10^{-6}$	36336	$1.66 \cdot 10^{-5}$	3601	$5.24 \cdot 10^{-5}$	3641	$1.53 \cdot 10^{-5}$	3662 $\cdot 10^{-6}$
	2	7158	$8.68 \cdot 10^{-7}$	7101	$9.53 \cdot 10^{-7}$	7009	$3.89 \cdot 10^{-7}$	7113	$9.47 \cdot 10^{-7}$	7154 $\cdot 10^{-7}$
	3	10483	$5.23 \cdot 10^{-8}$	10400	$6.15 \cdot 10^{-8}$	10215	$4.42 \cdot 10^{-8}$	10417	$6.13 \cdot 10^{-8}$	10473 $\cdot 10^{-8}$
	4	13652	$4.17 \cdot 10^{-9}$	13544	$6.53 \cdot 10^{-9}$	13240	$5.88 \cdot 10^{-9}$	13567	$6.32 \cdot 10^{-9}$	13635 $\cdot 10^{-9}$

Table S2: Theoretical wavenumbers in cm^{-1} for phenol obtained *via* the Numerov procedure at B3LYP/6-311++G(3df,3pd) level with and without GD3BJ dispersion correction. The deviations with respect to the experimental values in percent are given in parenthesis. The parameters k , d (in cm^{-1}) and R are obtained *via* linear regression between the experimental data (x-axis) and the respective theoretical values (y-axis).

		experimental	vacuum	implicit	explicit
CCl_4 B3LYP	ν_{01}	3612	3665 (1.47 %)	3637 (0.69 %)	3632 (0.55 %)
	ν_{02}	7055	7167 (1.59 %)	7111 (0.79 %)	7094 (0.55 %)
	ν_{03}	10327	10513 (1.80 %)	10431 (1.01 %)	10392 (0.63 %)
	ν_{04}	13435	13705 (2.01 %)	13599 (1.22 %)	13529 (0.70 %)
	k		1.022	1.014	1.008
	d		-34.91	-34.54	-10.53
	R		0.9999976	0.9999974	0.9999996
CCl_4 B3LYP + GD3BJ	ν_{01}	3612	3664 (1.44 %)	3636 (0.66 %)	3601 (0.30 %)
	ν_{02}	7055	7158 (1.47 %)	7101 (0.65 %)	7009 (0.65 %)
	ν_{03}	10327	10483 (1.52 %)	10400 (0.71 %)	10215 (1.08 %)
	ν_{04}	13435	13652 (1.62 %)	13544 (0.82 %)	13240 (1.46 %)
	k		1.017	1.009	0.981
	d		-11.76	-11.51	71.27
	R		0.9999995	0.9999993	0.99999926
n-Hexane B3LYP	ν_{01}	3622	3665 (1.19 %)	3642 (0.55 %)	3664 (1.15 %)
	ν_{02}	7074	7167 (1.31 %)	7122 (0.68 %)	7166 (1.30 %)
	ν_{03}	10358	10513 (1.50 %)	10447 (0.86 %)	10511 (1.47 %)
	ν_{04}	13472	13705 (1.73 %)	13621 (1.11 %)	13703 (1.71 %)
	k		1.019	1.013	1.019
	d		-34.68	-35.52	-35.33
	R		0.9999973	0.9999970	0.9999973
n-Hexane B3LYP + GD3BJ	ν_{01}	3622	3664 (1.16 %)	3641 (0.54 %)	3662 (1.11 %)
	ν_{02}	7074	7158 (1.20 %)	7113 (0.55 %)	7154 (1.13 %)
	ν_{03}	10358	10483 (1.22 %)	10417 (0.57 %)	10473 (1.11 %)
	ν_{04}	13472	13652 (1.34 %)	13566 (0.71 %)	13635 (1.21 %)
	k		1.014	1.008	1.012
	d		-11.52	-11.49	-6.46
	R		0.9999993	0.9999991	0.9999995

Table S3: Theoretical wavenumbers in cm^{-1} for 2,6-difluorophenol obtained *via* the Numerov procedure at B3LYP/6-311++G(3df,3pd) level. The deviations with respect to the experimental values in percent are given in parenthesis. The parameters k , d (in cm^{-1}) and R are obtained *via* linear regression between the experimental data (x-axis) and the respective theoretical values (y-axis).

		experimental	vacuum	implicit	explicit
CCl ₄	ν_{01}	3587	3639 (1.46 %)	3614 (0.76 %)	3599 (0.33 %)
	ν_{02}	7015	7119 (1.48 %)	7067 (0.74 %)	7029 (0.20 %)
	ν_{03}	10271	10443 (1.67 %)	10367 (0.93 %)	10294 (0.22 %)
	ν_{04}	13360	13616 (1.92 %)	13516 (1.17 %)	13396 (0.27 %)
	k		1.021	1.013	1.003
	d		-32.09	-29.66	-0.401
	R		0.9999963	0.9999964	0.9999996
n-Hexane	ν_{01}	3598	3639 (1.15 %)	3619 (0.59 %)	—
	ν_{02}	7028	7119 (1.29 %)	7077 (0.70 %)	—
	ν_{03}	10292	10443 (1.46 %)	10382 (0.88 %)	—
	ν_{04}	13395	13616 (1.65 %)	13536 (1.05 %)	—
	k		1.018	1.012	—
	d		-31.24	-29.34	—
	R		0.9999983	0.9999983	—

Table S4: Relevant distances and angles of the vacuum, implicit CCl_4 and explicit CCl_4 systems. The respective atom numbers are shown in Figure S2.

			vacuum	implicit	explicit
CCl ₄ B3LYP	$r(1 - 2)$	in Å	0.96	0.96	0.96
	$\alpha(3 - 1 - 2)$	in degree	109.88	109.93	110.35
	$r(1 - 17)$	in Å			3.09
	$r(1 - 18)$	in Å			4.85
	$\alpha(18 - 17 - 1)$	in degree			171.07
	$r(2 - 12)$	in Å			2.72
	$\alpha(1 - 2 - 12)$	in degree			144.95
	$r(2 - 15)$	in Å			3.92
	$\alpha(1 - 2 - 15)$	in degree			156.72
	$r(2 - 16)$	in Å			3.92
CCl ₄ B3LYP + GD3BJ	$\alpha(1 - 2 - 16)$	in degree			156.58
	$r(1 - 2)$	in Å	0.96	0.96	0.96
	$\alpha(3 - 1 - 2)$	in degree	109.78	109.83	110.21
	$r(1 - 17)$	in Å			3.06
	$r(1 - 18)$	in Å			4.70
	$\alpha(18 - 17 - 1)$	in degree			152.65
	$r(2 - 12)$	in Å			2.52
	$\alpha(1 - 2 - 12)$	in degree			159.06
	$r(2 - 15)$	in Å			3.69
	$\alpha(1 - 2 - 15)$	in degree			144.74
	$r(2 - 16)$	in Å			3.73
	$\alpha(1 - 2 - 16)$	in degree			146.36

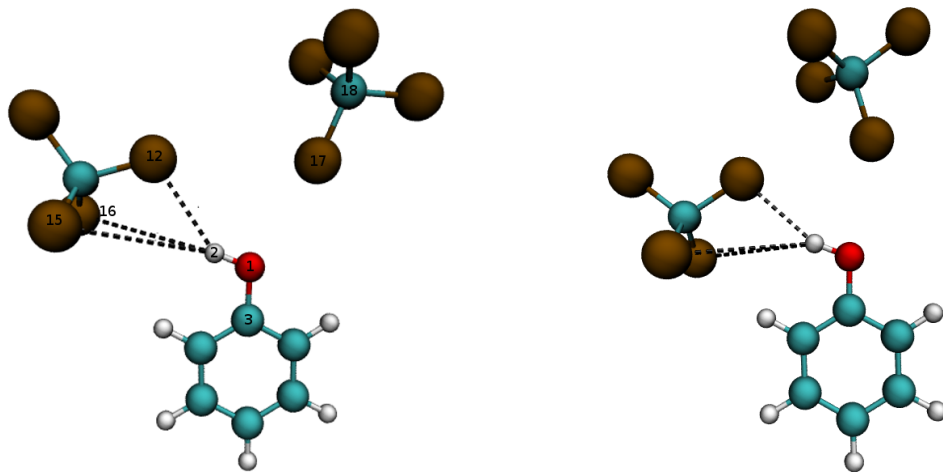


Figure S2: Structure of the explicit carbon tetrachloride system without (left) and with (right) GD3BJ dispersion correction applied.

Table S5: Structural data of the explicit n-hexane systems with and without dispersion correction.

			vacuum	implicit	explicit
n-Hexane B3LYP	$r(OH)$ $\alpha(COH)$	in Å ^a in degree	0.96 109.88	0.96 109.94	0.96 109.89
n-Hexane B3LYP + GD3BJ	$r(OH)$ $\alpha(COH)$	in Å ^a in degree	0.96 109.78	0.96 109.83	0.96 109.78

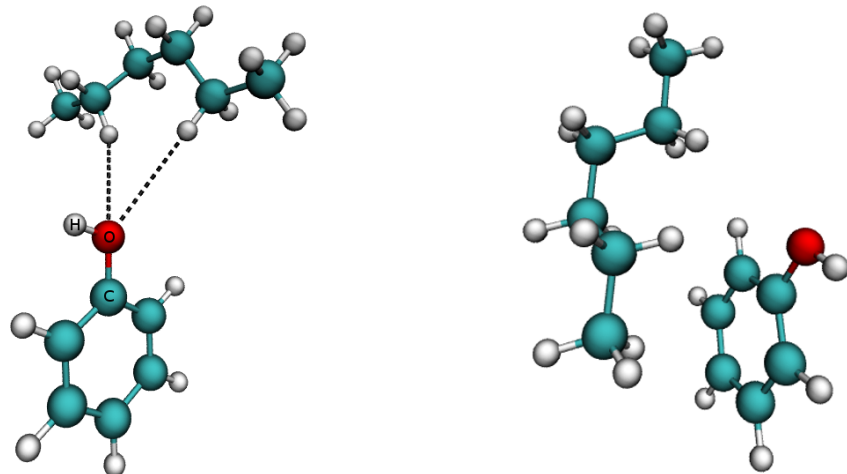


Figure S3: Structures of the explicit n-hexane system with (right) and without (left) dispersion correction. Due to the very weak interaction energies the explicit n-hexane system geometry is very sensitive to dispersion correction, shifting the n-hexane molecule towards the aromatic moiety.